



Cite this: *Mol. Syst. Des. Eng.*, 2024, **9**, 561

Formation mechanism of anisotropic gelatin hydrogel by self-assembly on oriented templates†

Kohei Kawaguchi,^a Tamaki Maeda,^a Syuuhei Komatsu,^b Yoshihiro Nomura^c and Kazuki Murai ^{*a}

The development of structurally controlled techniques inspired by the structural formation of living systems is of great importance for the fabrication of next-generation functional soft materials using environmentally friendly processes. This study aimed to investigate the formation mechanism of anisotropic structures of the gelatin network in a hydrogel through self-assembly on oriented templates. The effects of the oriented template having a uniaxially oriented surface on the anisotropic structure of the gelatin network were influenced by the structure at different scales: molecular (the secondary structure as the microstructure on the gelatin molecule) and molecular-assembled (the morphology of the gelatin network) scales. The mechanical properties and swelling behavior of the prepared gelatin hydrogels were characterized based on the anisotropic gelatin networks. The formation of an anisotropic gelatin network by self-assembly on the oriented template was presumably achieved by a two-step process due to the following two types of structural control factors: (1) the strength of the interaction between the template and gelatin molecules, and (2) the phase separation between the gelatin and water molecules induced during the hydrogelation process. The first process involves the formation of a thin molecular layer by the interaction between the template and gelatin molecules. The second process involves phase separation between the gelatin and water molecules during the cooling process of hydrogelation. These structurally controlled techniques for the formation of polymer networks inspired by biomineralization have two application prospects, which are the construction of biological tissue-like soft materials with complex hierarchical and anisotropic network structures through self-assembly processes, and expression of biological tissue-like functions.

Received 1st February 2024,
Accepted 12th March 2024

DOI: 10.1039/d4me00023d

rsc.li/molecular-engineering

Design, System, Application

The development of structurally controlled techniques inspired by the structural formation of living systems is of great importance for the fabrication of next-generation functional soft materials using environmentally friendly processes. Our study aims to clarify the formation mechanism of anisotropic gelatin networks on the templates by examining between the gelatin molecules and the template surface, as well as the time-dependent formation and growth of the gelatin network during hydrogelation. The formation and growth of the anisotropic gelatin network was achieved by self-assembly on oriented templates in a two-step processes. The first process involves the formation of a thin molecular layer through the interaction between the template and gelatin or water molecules in the aqueous solution. The second process is phase separation between gelatin and water molecules during hydrogelation. Knowledge of the formation and growth mechanisms of anisotropic polymer networks by self-assembly is expected to trigger innovations in the field of nanotechnology, including the fabrication of functional soft materials and self-organizing nanomaterials using bioinspired processes.

Introduction

A hydrogel is a type of soft matter with a high water content in three-dimensional (3D) networks with crosslinked structures between polymers. There has been significant interest in the functional design of hydrogels through structural control of polymers and polymer networks, as evidenced by the numerous attractive hydrogels that have been reported, including nanocomposite gels and instant thermal switching hydrogels.^{1–6} These hydrogels possess unique features, such as structural color and enhanced mechanical properties, which are inspired by the

^a Department of Chemistry and Materials, Faculty of Textile Science and Technology, Shinshu University, 3-15-1 Tokida, Ueda, Nagano 386-8567, Japan. E-mail: murai_kazuki@shinshu-u.ac.jp

^b Department of Materials Science and Technology, Faculty of Advanced Engineering, Tokyo University of Science, 6-3-1 Niijuku, Katsushika-ku, Tokyo 125-8585, Japan

^c Scleroprotein and Leather Research Institute, Faculty of Agriculture, Tokyo University of Agriculture and Technology, 3-5-8, Saiwai-cho, Fuchu, Tokyo 183-8509, Japan

† Electronic supplementary information (ESI) available: AFM images of the oriented and non-oriented templates, TG-DTA profiles of the prepared hydrogels, and swelling behavior of the prepared hydrogels at several cooling rates. See DOI: <https://doi.org/10.1039/d4me00023d>

nanostructures of biological tissues. In particular, the hierarchically ordered structures found in biological soft tissues (e.g., muscles and cartilages)^{7,8} play important roles in inducing biological functions. Interestingly, these 3D structures are formed through self-organization at scales ranging from nanometers to micrometers. Therefore, developing structurally controlled techniques inspired by the structural formation of living systems is important for the fabrication of next-generation functional hydrogels using environmentally friendly processes. Gelatin hydrogel is one of the most widely studied soft matters and is used in a range of research fields, including biology, engineering, and food science.^{9–12} However, gelatin hydrogels with orientation and hierarchy by self-assembly have not been reported. Gelatin is a heat-denatured protein that loses its ability to self-assemble from collagen upon heat treatment. We recently reported primary results on the fabrication of hydrogels with anisotropic gelatin networks in a uniaxial direction using an oriented template,^{13,14} which was inspired by the structural control of bioinorganic materials during biomineralization. We defined a template with a uniaxially oriented surface as the oriented template, while the non-oriented template was defined as a template with non-oriented surface in these studies. While structural control of inorganic materials during biomineralization has been reported in numerous studies,^{15–20} the structural control of organic polymers inspired by biomineralization has not been previously reported. Therefore, the development of a universal structure control technology for organic polymers, inspired by the principle of structure control for inorganic materials in biomineralization, is a promising prospect. However, this could not be achieved due to the lack of understanding of the formation mechanism of anisotropic gelatin networks by self-assembly on a template. This study aims to clarify the formation mechanism of anisotropic gelatin networks on the templates by examining between the gelatin molecules and the template surface, as well as the time-dependent formation and growth of the gelatin network during hydrogelation. Novel structural control factors are also proposed for the anisotropic growth of polymer networks during hydrogelation.

Experimental

Preparation of gelatin hydrogels and evaluation of swelling behavior

Anisotropic and isotropic gelatin hydrogels were prepared using a facile fabrication method according to a previously reported method.¹³ Gelatin from bovine skin (type B) was dissolved in ultrapure water and incubated at 37 °C. The gelatin solution concentration was fixed at 10 wt%. The gelatin solution was introduced into a reaction cell containing two glass substrates (10 cm × 10 cm) separated by a 2.0 mm silicon spacer. To induce anisotropic growth of the gelatin networks, polypropylene (PP), polyvinyl chloride (PVC), and Al sheet-coated glass substrates were used as

oriented templates for structural control. Hydrogelation was achieved by cooling the reaction cell filled with the gelatin solution at 4 °C. The prepared sheet-shaped hydrogels were carefully removed from the reaction cell and cut into disk-shaped hydrogels (10.00 mm (diameter [d]) × 2.00 mm (thickness [z])). The as-prepared hydrogels were immersed in cold water to achieve equilibrium swelling and stored in cold water until measurement.

To evaluate the swelling behavior of the hydrogels, the as-prepared disk-shaped hydrogels were immediately immersed in cold water to induce spontaneous swelling, and their diameters and thicknesses were measured every 20 min. The percentage swelling rate of the hydrogels was calculated using eqn (1):

$$\text{Swelling rate } (d/d_0, z/z_0) = \frac{[d] \text{ or } [z]}{[d_0] \text{ or } [z_0]} \times 100 \quad (1)$$

where [d_0] and [d] are the diameters of the hydrogels before and after swelling, respectively, and [z_0] and [z] are the hydrogel thicknesses before and after swelling, respectively.

Compression tests and rheological evaluation

Compression tests were performed to examine the mechanical properties of the anisotropic and isotropic gelatin hydrogels using thermomechanical analysis (TMA; Hitachi TMA/SS6100). The compression speed was set to 500 $\mu\text{m min}^{-1}$, and a quartz probe was used for compression. The swollen disk-shaped hydrogels were compressed perpendicularly to a disk surface at a temperature of 25 °C.

The swollen hydrogels in the equilibrium swelling state were rheologically evaluated using a parallel-plate rheometer (Malvern, Kinexus Pro, diameter: 20 mm, gap: 2.5 mm). The storage elastic modulus (G') and loss elastic modulus (G'') were measured in an angular frequency of 0.1–10.0 rad s^{-1} , a constant strain of 0.1%, and temperature of 20 °C.

Thermogravimetric-differential thermal analysis

The water and gelatin compositions in the swollen gelatin hydrogels were determined using thermogravimetric-differential thermal analysis (TG-DTA) on a Thermo plus TG 8120 (Rigaku) apparatus at a rate of 10 °C min^{-1} and temperatures of 20–1000 °C.

Scanning electron microscopy and atomic force microscopy observations

The morphologies of the gelatin networks at the surface and cross-sections were observed using a scanning electron microscope (SEM, Hitachi S-3000N) at an accelerating voltage of 20 kV and an emission current of 30 μA . The swollen hydrogels were cut to expose the surface and cross-sections and then lyophilized. The dried gel samples were coated with Pt nanoparticles by ion sputtering.

The nanostructure on the surface of the templates and the morphology of the gelatin assembly adsorbed on the substrates were observed using atomic force microscopy

Table 1 Water contact angles of the pristine and gelatin-adsorbed templates

Samples	Contact angle/deg.
PP template	87.4 ± 0.2
PVC template	84.9 ± 2.4
Al template	84.6 ± 1.0
Glass template	44.4 ± 3.1
Gelatin-PP	77.2 ± 2.7
Gelatin-PVC	84.3 ± 0.0
Gelatin-Al	84.9 ± 2.0
Gelatin-glass	48.0 ± 1.5

(AFM, Hitachi AFM5200S). AFM observations were conducted in the dynamic force mode at 25 °C in air. Samples for AFM observation were prepared by casting approximately 100 μL of 0.1 wt% gelatin solution onto the substrates and incubating them for 5 min, 10 min, and 30 min at 37 °C. Following incubation, the substrates were washed with ultrapure water. Gelatin networks on the substrates were fixed by cooling at 4 °C. The substrates were then dried in air.

Contact angle measurement

The surface properties of the templates were evaluated through contact angle measurements using an auto-contact

angle meter (DMS-400, Kyowa Interface Science). In addition, changes in the surface properties of the templates after casting the gelatin solution on the substrates were evaluated using contact angle measurements. Samples of the gelatin-adsorbed templates were prepared using the same method used for the AFM observation.

Results and discussion

Structural analysis of the gelatin networks in hydrogels

Gelatin hydrogels were prepared on four different templates: PP, PVC, and Al sheet-coated substrates (oriented templates) and a glass substrate (non-oriented template: control). The surface morphologies of the PP-, PVC-, and Al-oriented templates were examined using AFM. The templates exhibited a uniaxially oriented structure (Fig. S1a–c†), whereas the surface morphology of the glass template showed a non-oriented surface structure and microscale of craters (Fig. S1d†). The surface properties of the pristine templates were evaluated using water contact angle measurements (Table 1). The surface of the glass template had a lower contact angle than those of the other templates. These indicate that the PP, PVC, and Al templates have more oriented structures and hydrophobic surfaces than the glass template.

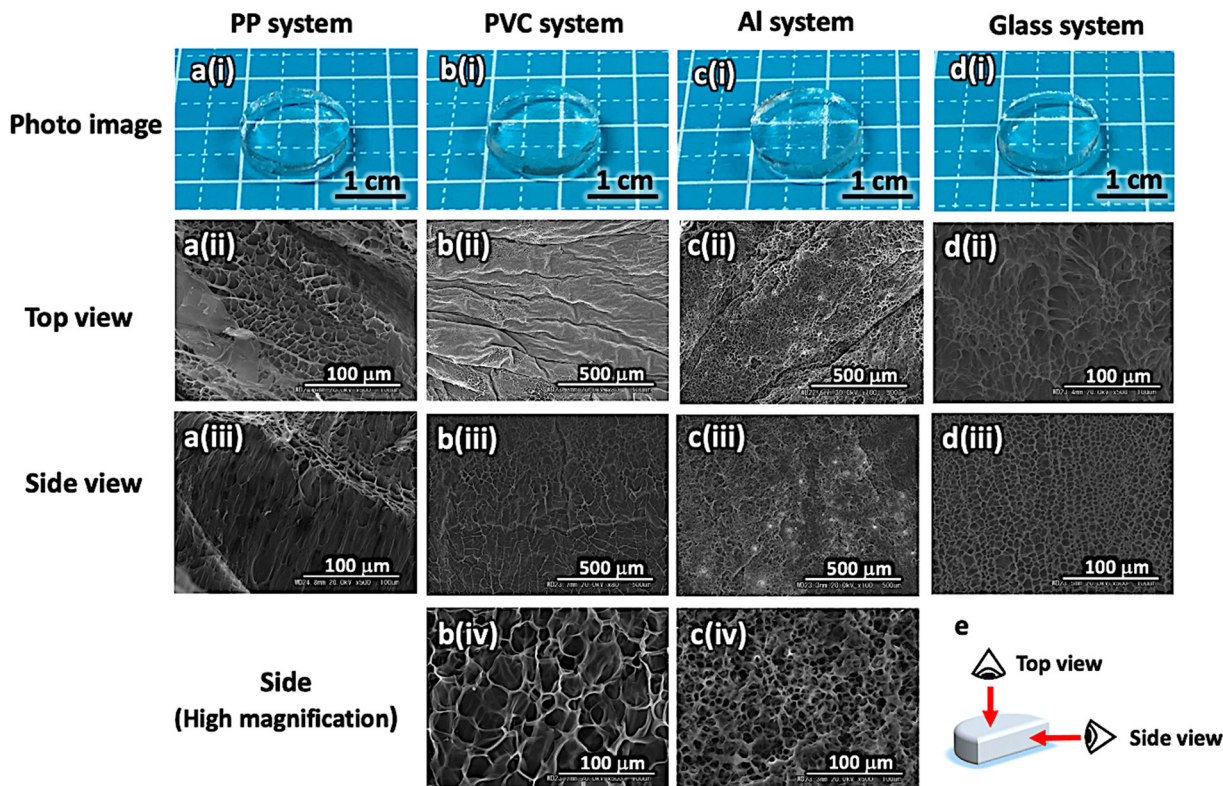


Fig. 1 Appearance of the prepared gelatin hydrogels (i) and SEM images of the gelatin networks observed from the top (ii) and side views (iii and iv). a–d) Templates used to prepare the hydrogels. b(iv) and c(iv) High-magnification SEM images corresponding to b(iii) and c(iii), respectively. e) Viewpoints of the SEM observations.

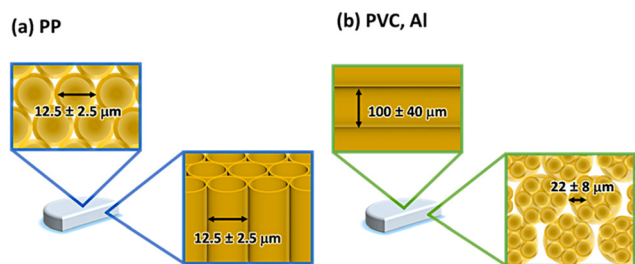
Table 2 Summary of the composition and mechanical properties of hydrogels prepared using each system. The error ranges were calculated from the data for the three samples

Samples		PP system	PVC system	Al system	Glass system
Composition/wt%	Gelatin	5.6 ± 0.4	4.6 ± 0.4	4.8 ± 0.8	4.8 ± 0.4
	Water	94.4 ± 0.4	95.4 ± 0.4	95.2 ± 0.8	95.2 ± 0.4
Young's modulus/kPa		43.5 ± 3.9	18.4 ± 1.7	18.7 ± 2.6	40.0 ± 5.2
Fracture stress/kPa		25.1 ± 2.7	6.5 ± 2.4	5.6 ± 1.7	19.1 ± 0.7
Fracture strain/m m ⁻¹		0.568 ± 0.013	0.277 ± 0.092	0.266 ± 0.067	0.581 ± 0.051

The prepared hydrogels were transparent and colorless in all systems (Fig. 1(i)). The hydrogel components were determined using TG-DTA measurements (Fig. S2†). The results are summarized in Table 2. The hydrogels prepared in all systems had the same water content (>90 wt%). The morphology of the gelatin networks in the hydrogels was investigated by SEM (Fig. 1(ii)–(iv)) from two views (top view: gel surface, side view: gel cross-section) (Fig. 1e). The gelatin networks in the hydrogel prepared using the glass system exhibited an isotropic 3D structure with the same morphology in the top and side views (Fig. 1d(ii) and (iii)). The morphologies of the gelatin networks of the hydrogels prepared in the PP, PVC, and Al systems varied depending on the observational viewpoints. The morphology of the gelatin network observed in the PP system was porous, as shown in the top view (Fig. 1a(ii)), whereas that in the side view was a tube-like structure perpendicular to the surface of the disk hydrogel (Fig. 1a(iii)). The growth direction of the tube-like gelatin network corresponded to that perpendicular to the oriented surface nanostructure of the PP template. Conversely, in the PVC and Al systems, the prepared hydrogels were observed as both tube-like networks in the top view and porous structures in the side view (Fig. 1b(ii)–(iv) and c(ii)–(iv)). The growth direction of the tube-like networks in the PVC and Al systems matched the orientation direction of the surface nanostructures on the PVC and Al templates. These results indicate that the growth direction of the anisotropic gelatin network in the hydrogel is structurally controlled by factors other than the surface nanostructure of the oriented template. Interestingly, the diameters of the tube-like networks formed in the PVC and Al systems were different in the top and side views. From the top view, the diameters of the tube-like networks were 100 ± 40 μm (PVC

system) and 100 ± 50 μm (Al system), whereas from the side view, the pore sizes of the tube-like networks were 22 ± 8 μm and 7 ± 4 μm, respectively. These values were calculated using SEM observational analysis (Fig. 1b(iv) and c(iv)). The gelatin networks observed in the PVC and Al systems were presumably formed by the assembly of numerous gelatin tube-like structures (Fig. 2). The presence of anisotropic structures in the gelatin networks with different growth directions suggests that biomineralization-inspired template-based methods can control the molecular-assembled morphology of organic polymers. Therefore, these results imply that the oriented templates not only impact the growth direction and morphology of the gelatin networks, but also the formation of the assembled structure.

We focused not only on the morphological changes in the gelatin network at the macroscale, but also on changes in the secondary structure of the gelatin molecule at the microscale before and after hydrogelation. We analyzed the secondary structure of gelatin using peak deconvolution of the attenuated total reflection Fourier transform infrared (ATR-FTIR) spectra, which were obtained by lyophilizing the prepared hydrogels in each system. The analytical results for the secondary structures of the pristine gelatin and gelatin in the prepared hydrogels for each system are summarized in Table 3. The secondary structure of gelatin in the anisotropic hydrogels changed significantly compared with those of the pristine gelatin and the gelatin in the isotropic hydrogel due to an increase in α-helical structure content. Therefore, these results indicate that the oriented template controls the structure at different scales, including the secondary structure (molecular scale) as a microstructure on gelatin molecules and the morphology of the gelatin network (molecular-assembled scale) as a macrostructure.

**Fig. 2** Oriented structure of tube-like gelatin networks in hydrogels prepared using the (a) PP and (b) PVC and Al systems.**Table 3** Summary of the secondary structure of gelatin under each condition. The error ranges were calculated from the data for the three samples

Samples	Content/%		
	α-Helix	β-Sheet	Random coil
Pristine	35.4 ± 1.6	51.3 ± 0.4	13.3 ± 1.2
Glass system	34.9 ± 0.1	52.5 ± 1.1	12.6 ± 1.2
PP system	64.3 ± 0.6	29.4 ± 0.6	6.3 ± 0.3
PVC system	51.1 ± 0.7	38.5 ± 0.4	10.4 ± 0.3
Al system	51.6 ± 1.5	37.2 ± 1.5	11.2 ± 0.2

Influence of the anisotropic gelatin networks on the gel properties

To explore the influence of anisotropic gelatin networks on hydrogel properties, we investigated the swelling behavior of the prepared hydrogels in water. We measured the swelling behavior using a disk-shaped hydrogel (diameter [d]: 10.00 mm, thickness [z]: 2.00 mm) at 20 min intervals and calculated the swelling rate using eqn (1). Different swelling behaviors of the hydrogels were observed depending on the specific gelatin networks. In particular, the PP, PVC, and Al systems with anisotropic gelatin networks exhibited anisotropic swelling behavior in the [d] or [z] axial directions (Fig. 3a). The hydrogels with gelatin networks grown perpendicular to the disk-hydrogel surface (PP system) exhibited higher swelling behavior along the [d] axis than along the [z] axis. The swelling rates along the [d] and [z] axes after 300 min were $128 \pm 3\%$ and $111 \pm 1\%$, respectively. However, hydrogels with gelatin networks grown in the direction parallel to the disk-hydrogel surface (PVC and Al systems) showed a high swelling rate along the [z] axis. The swelling rates in the [d] and [z] axes after 300 min of hydrogels prepared in the PVC system were $140 \pm 4\%$ and $150 \pm 3\%$, respectively, whereas those in the Al system were $140 \pm 5\%$ and $147 \pm 9\%$, respectively. In contrast, the hydrogel with an isotropic gelatin network (glass system) exhibited isotropic swelling behavior in the [d] and [z] axes, with swelling rates of $125 \pm 5\%$, and $125 \pm 10\%$, respectively, after 300 min. These results indicate that the swelling axis of the anisotropic hydrogels was perpendicular to the orientation direction of the gelatin tube-like networks. We speculate that anisotropic hydrogels (PP, PVC, and Al

systems) have dense gelatin molecules aligned in the direction of the tube-like networks, while the direction perpendicular to the tube-like networks has only low-density assemblies due to gelatin network interactions. Therefore, the axial direction perpendicular to the tube-like networks would induce high swelling compared to the axial direction of the tube-like networks. Thus, the hydrogels with tube-like networks swelled in the direction perpendicular to the tube-like networks (Fig. 3b). Interestingly, the hydrogels prepared in the PVC and Al systems demonstrated higher swelling rates compared to those in other systems. This suggests that the interaction between the axial direction perpendicular to the tube-like networks in the hydrogels prepared in the PVC and Al systems was weaker than that of other hydrogels. Consequently, the hydrogels prepared in the PVC and Al systems exhibited a high swelling ratio with water molecules in the space between the tube-like networks.

Next, we assessed the mechanical properties of the hydrogels using compression tests performed in the direction perpendicular to the surface of the disk-shaped hydrogel. Fig. 4a shows the stress–strain curves of the isotropic and anisotropic hydrogels. The mechanical properties of the hydrogels varied across systems due to the differences in the anisotropic gelatin networks (Table 2). The Young's modulus and fracture stress of the anisotropic hydrogel prepared in the PP system, which had an oriented tube-like network perpendicular to the compression plane, were higher than those of the other anisotropic (PVC and Al systems) and isotropic hydrogels. However, these values decreased in the anisotropic hydrogels (PVC and Al systems) with an oriented tube-like network parallel to the compression plane. Therefore, the anisotropic hydrogel (PP system), which has oriented tube-like networks corresponding to the compression direction, requires a large stress to deform compared with other anisotropic (PVC and Al systems) and isotropic hydrogels (Fig. 4b). In addition, we conducted dynamic viscoelastic measurements of the prepared hydrogels using a rheometer and confirmed the difference in rheological properties between the anisotropic and isotropic gelatin hydrogels (Fig. 4c). The storage elastic modulus (G') of the anisotropic hydrogels was greater than that of the isotropic gelatin hydrogels in many angular frequency ranges. We believe that this difference was induced by the presence of a specific structure formed by the gelatin network in the anisotropic hydrogel. These findings confirm the presence of an anisotropic gelatin network in the hydrogel prepared by self-assembly.

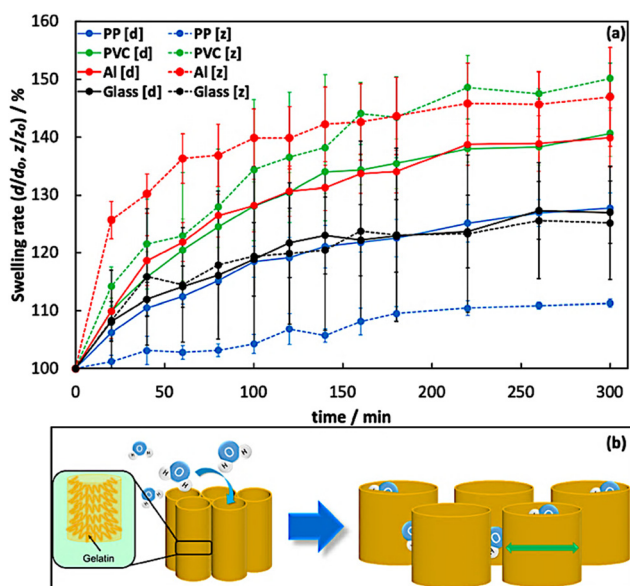


Fig. 3 (a) Swelling rates of the hydrogels prepared at each system obtained through measurements conducted in water at 4 °C. (b) Anisotropic swelling mechanism of tube-like networks in the prepared hydrogels. The swelling test was performed three times.

Analysis of interaction between template and gelatin molecules

In this study, we revealed that the orientational direction of gelatin networks in an anisotropic hydrogel differed by hydrogelation on oriented templates with a similar surficial nanostructure. To investigate the early stages of network formation, we examined time-dependent morphological

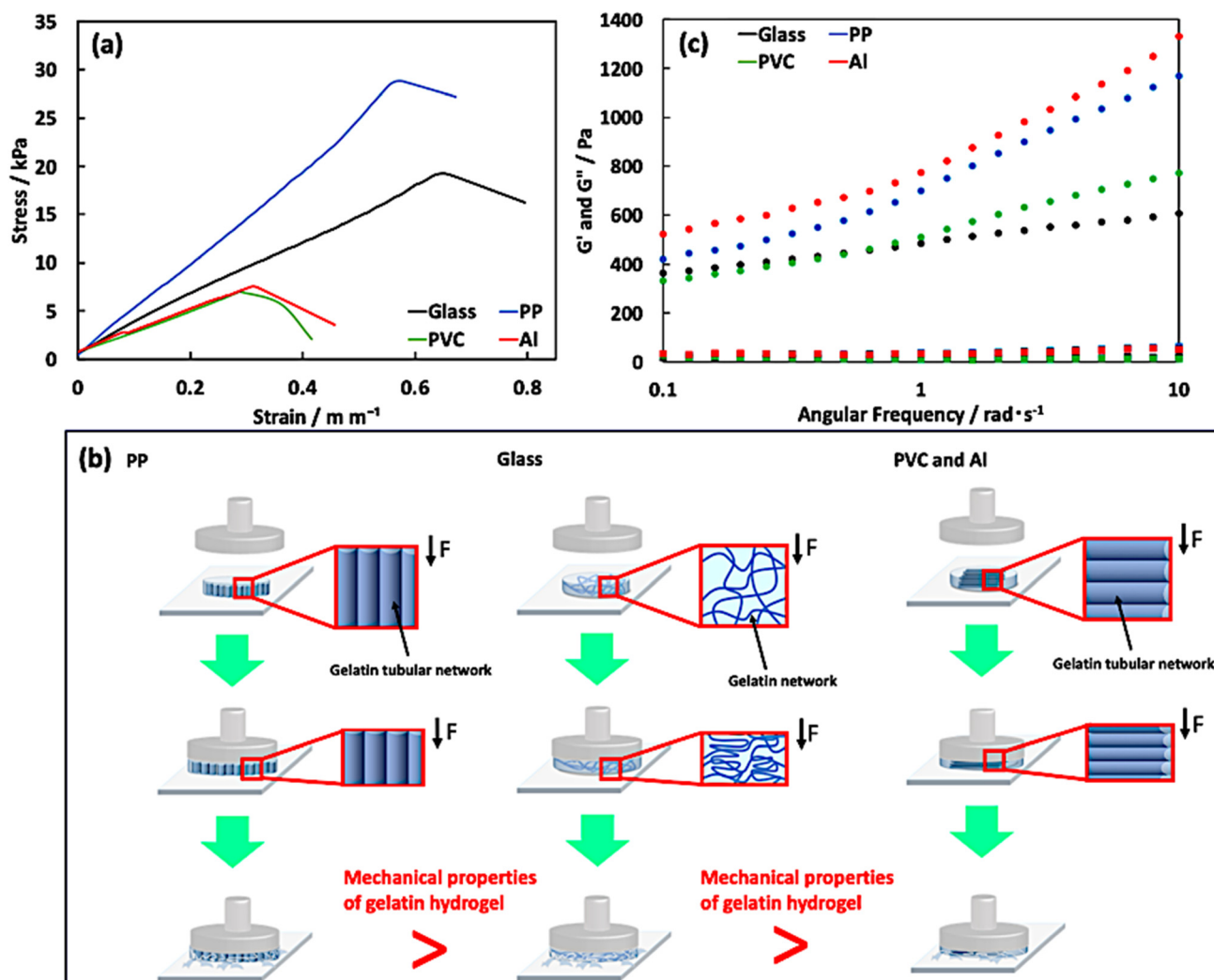


Fig. 4 Analysis of the (a) mechanical and (c) viscoelastic properties of the prepared hydrogels in each system. Stress–strain curves of the hydrogels prepared at each system obtained by conducting a compression test at 25 °C for thermomechanical analysis. The compression test was performed thrice. (b) Schematic images of the behavior of gelatin networks in the hydrogels prepared in the PP, glass, PVC and Al systems during the compression test.

changes in the gelatin assembly absorbed on the templates using AFM. Fig. 5 shows the AFM images of the gelatin assembly formed on the template surface after several incubation times (5, 10, and 30 min). The AFM images reveal that the adsorbed region and morphology of the gelatin assembly differed depending on the template. The PP system formed and densified the gelatin assembly over a wide region with increasing incubation time. However, the height (75 ± 25 nm) and width (13 ± 2 nm) of the gelatin assembly remained unchanged. These results suggest that the gelatin molecules not only interact well with the PP template but also form a dense assembly by actively approaching the PP template surface. However, the PVC and Al systems not only formed gelatin assemblies that only interact well with the PP template but also formed a dense assembly by actively approaching the PP template surface. However, the PVC and Al systems formed gelatin assemblies in only a very small region. In addition,

the gelatin assembly did not show additional formation or growth with increasing incubation time. Furthermore, no gelatin assembly was observed on the template in the glass system at any incubation time. The PP system demonstrated a stronger interaction between template and gelatin molecules compared to the other systems. The non-adsorption of gelatin molecules on the template in the glass system is believed to be a result of the preferential interaction of the glass template with water molecules, owing to its highly hydrophilic surface compared to the other templates. Hence, we speculate that the formation of a thin layer of water on the glass template surface inhibits the interaction between the template and gelatin molecules. Moreover, the formation of a gelatin assembly over a wide region induced a change in the surface properties of the PP template, which was investigated using water contact angle measurements (Table 1). When the gelatin assembly was formed on the PP template, the water contact angle at

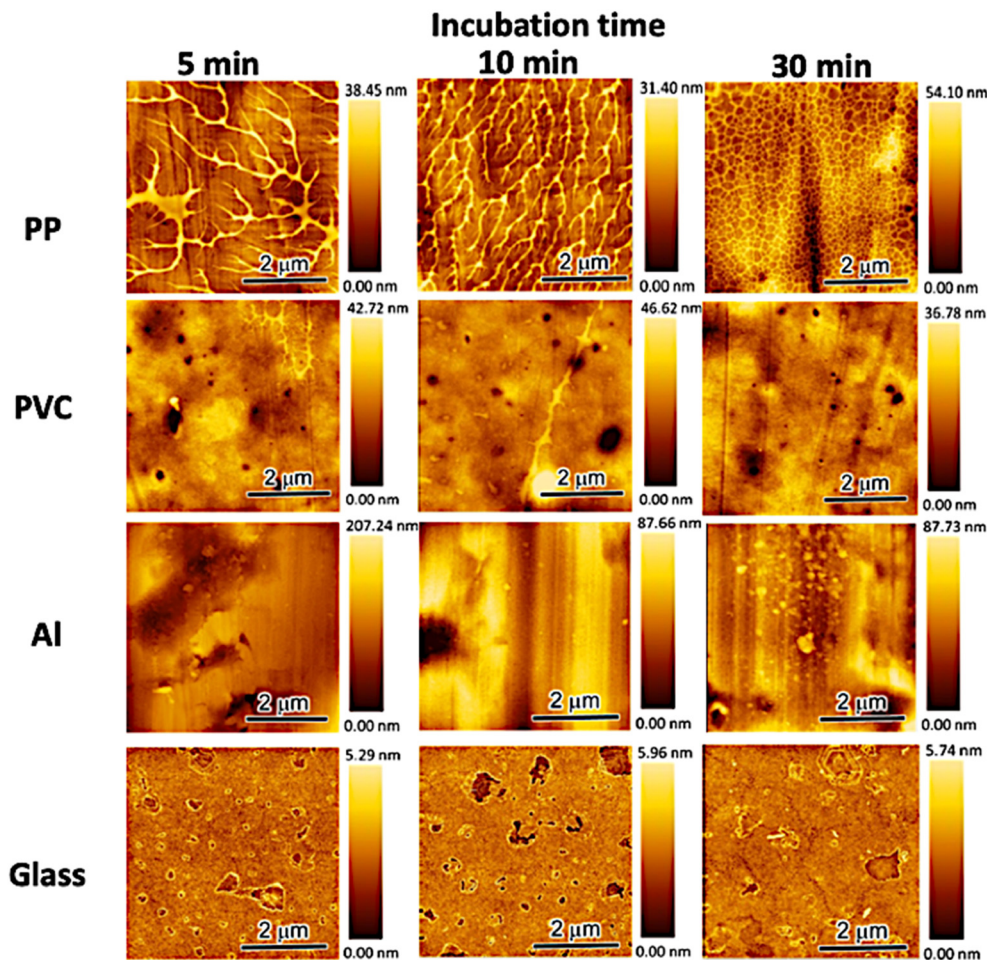


Fig. 5 Dynamic changes in the morphology of the gelatin assembly formed on the substrate surface after casting a 0.1 wt% gelatin aqueous solution.

the surface of the gelatin absorbed PP template was lower than that of the pristine PP template. On the other hand, other systems did not display any change in the contact angle of water compared to the pristine templates. This suggests that the PP template surface was hydrophilized by the gelatin assembly. Furthermore, the AFM results imply the existence of strong interactions between the gelatin molecules and the template in the PP system, whereas the interactions between other templates and gelatin molecules are weak or negligible. These results indicate that the surface properties of the template influenced the adsorption of gelatin molecules and the formation of gelatin assemblies on the template.

The assembly of gelatin molecules during cooling is important for hydrogelation using a gelatin solution. Hence, we investigated the influence of different cooling rates on the formation of anisotropic gelatin networks for the hydrogelation of gelatin solutions. Fig. 6 shows the change in swelling ratio of the prepared hydrogels at eight different cooling rates (80, 40, 30, 20, 15, 10, 5, and 3 °C h⁻¹). This swelling test was performed on the prepared hydrogels with a thickness of 5 mm because of the

formation of anisotropic gelatin networks due to differences in the cooling rates. The swelling ratios of the hydrogels were calculated using eqn (2):

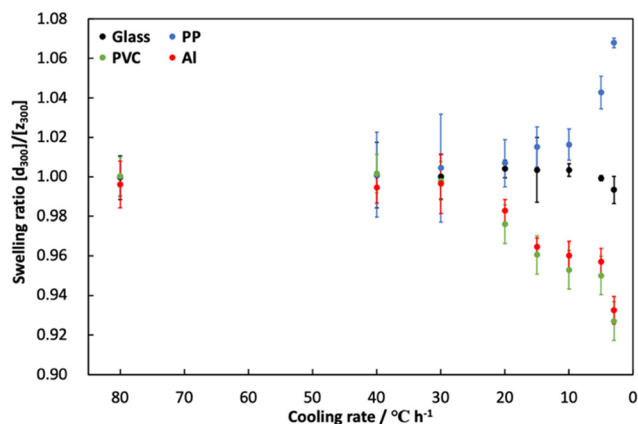


Fig. 6 Changes in the swelling ratio of gelatin hydrogels prepared at different cooling rates. Swelling tests were performed using the prepared hydrogels having 5 mm of thickness.

$$\text{Swelling ratio } (d_{300}/z_{300}) = \frac{[d_{300}]}{[z_{300}]} \times 100 \quad (2)$$

where $[d_{300}]$ and $[z_{300}]$ are the diameter and thickness of the hydrogels after swelling for 300 min, respectively. The swelling behaviors of the prepared hydrogels are summarized in Fig. S3.† The swelling ratio of the prepared hydrogels at all cooling rates in the glass system was approximately 1.00. This result indicates that the prepared hydrogels had an isotropic gelatin network regardless of the cooling rate. By contrast, the swelling ratios of the hydrogels prepared in the PP, PVC, and Al systems were significantly influenced by the cooling rate used for hydrogel formation. The swelling ratios of hydrogels prepared at rapid cooling rates (80, 40, and 30 °C h⁻¹ and 20 °C h⁻¹ for the PP system only) were approximately 1.00, which is similar to that of the hydrogel prepared in the glass system. This suggests that the gelatin networks in hydrogels prepared in the PP, PVC, and Al systems did not exhibit anisotropy at rapid cooling rates. On the other hand, the swelling ratios of the prepared hydrogels at slow cooling rates (20 °C h⁻¹ for the PVC and Al systems, and 15, 10, 5, and 3 °C h⁻¹ for all systems) changed exponentially with decreasing cooling rate. In particular, we observed that the swelling ratio of the hydrogel prepared in

the PP system increased with a decreasing cooling rate. This indicates that the hydrogel swelled preferentially in the diametric direction $[d]$ compared to the thickness direction $[z]$. However, the swelling ratios of the hydrogels prepared in the PVC and Al systems decreased with an increasing cooling rate, indicating that the hydrogels swelled preferentially in the thickness direction $[z]$ than the diametric direction $[d]$. These swelling behaviors indicate that when the cooling rate was reduced during the hydrogelation process, the gelatin network in the hydrogel exhibited anisotropy and formed a more ordered structure. We believe that the high anisotropy of the gelatin network was induced by accurate phase separation between gelatin and water molecules using the gelatin assembly formed on the anisotropic templates at a slow cooling rate.

Anisotropic growth mechanisms of the gelatin networks on the oriented templates

We confirmed the presence of an anisotropic gelatin network, as evidenced by SEM observations, swelling behavior, and mechanical properties of the hydrogel. In this section, we discuss the anisotropic growth mechanisms of the gelatin network through self-assembly on the templates. To explain the formation and growth mechanisms of anisotropic gelatin

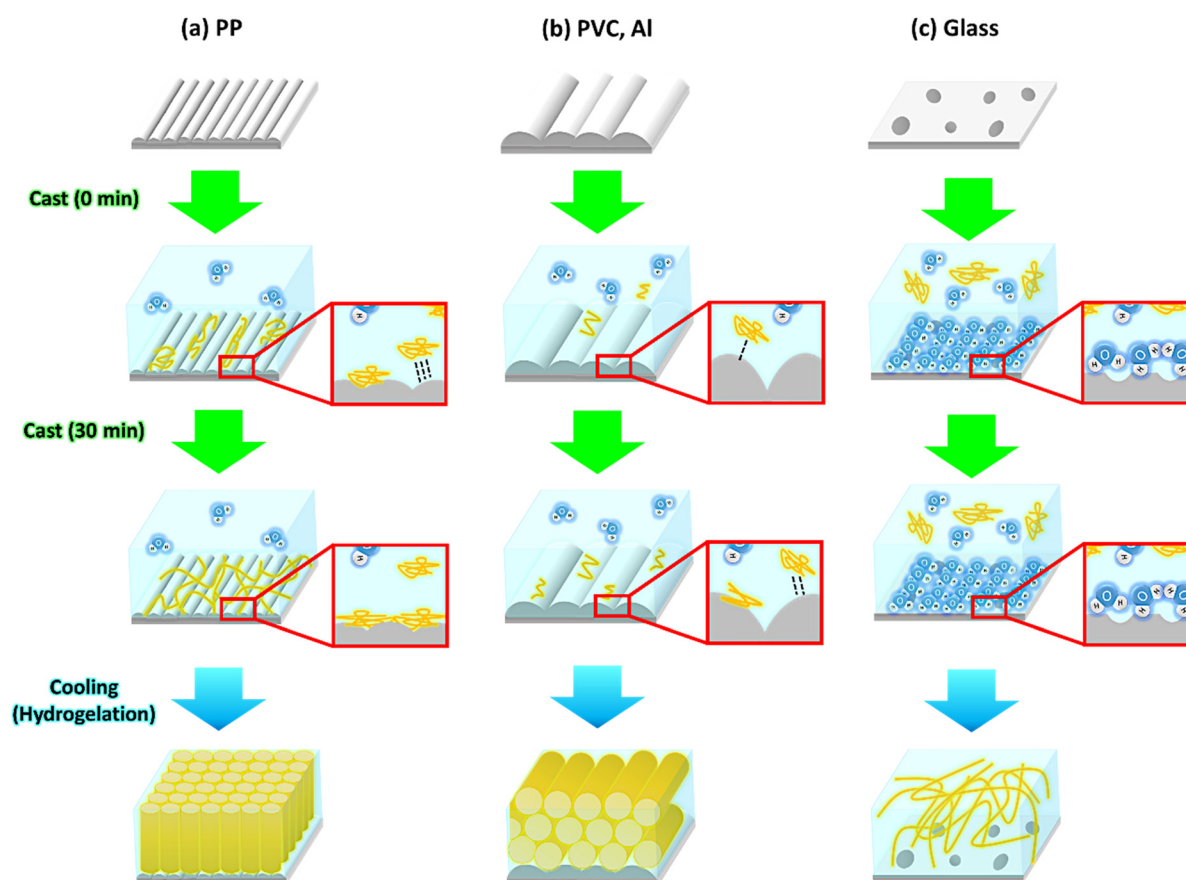


Fig. 7 Schematic illustration of formation mechanisms of oriented gelatin networks on (a) PP, (b) PVC and Al, and (c) glass templates.

networks by self-assembly, we focused on two factors: (1) the strength of the interaction between the template and gelatin molecules and (2) the phase separation between the gelatin and water molecules induced during the hydrogelation process. Based on our experimental results, we propose that the anisotropic structure of the gelatin network in the oriented template systems was formed through a two-step process (Fig. 7). The first step involves the formation of a thin molecular layer *via* the interaction between the template and gelatin or water molecules in the aqueous solution. The strength of this interaction depends on the surface properties of the template, and the difference in the strength and existence of the interaction affects the adsorption of gelatin molecules onto the template and the formation of gelatin assemblies. AFM observations and contact angle measurements showed that the surface of the PP template strongly interacted with the gelatin molecules, inducing the adsorption of gelatin molecules and the formation of a wide region of a thin gelatin layer on the template. The formed thin gelatin layer plays an important role in the anisotropic growth of gelatin networks by phase separation during hydrogelation, which is the second process. In contrast, other templates exhibited weak or no interactions between the gelatin molecules and the templates. Because the glass template is hydrophilicity compared to other templates, the glass system preferentially interacts with water molecules. Therefore, in the glass system, the formation of a thin layer of gelatin networks is inhibited, and specific growth of the networks does not occur. The second process involves phase separation between the gelatin and water molecules during the cooling process of hydrogelation. This separation was induced when the template surface was cooled, resulting in the formation of a gelatin assembly at the template surface, which acted as a precursor network for the anisotropic growth of tube-like networks. In contrast, PVC and Al systems have weak interactions between the gelatin molecules and hydrophobic template surface. Hence, the preferential interaction between the water molecules and the template is the same as that of the glass system. These factors affect the phase separation between the gelatin and water molecules induced by the hydrogelation process, which is achieved by cooling the gelatin aqueous solution. The results of the AFM observations showed that the gelatin molecules were adsorbed onto the PVC and Al template surfaces (Fig. 5). Moreover, phase separation during the hydrogelation process occurs at the template surface, on which gelatin molecules are slightly adsorbed. Hence, we speculate that anisotropic growth of the gelatin network was induced along the oriented structure of the PVC and Al template surfaces. As a result, gelatin molecules without the ability to self-assemble formed a 3D network with various orientations *via* hydrogelation.

Conclusion

The formation and growth of an anisotropic gelatin network was achieved by self-assembly on oriented templates in a

two-step processes. The first process involves the formation of a thin molecular layer through the interaction between the template and gelatin or water molecules in the aqueous solution. The second process is phase separation between gelatin and water molecules during hydrogelation. Therefore, the structure of the gelatin networks is influenced by two factors: (1) the strength of the interaction between the template and gelatin molecules, and (2) the phase separation of gelatin molecules induced by hydrogelation. The anisotropic gelatin networks induced anisotropic swelling behavior and mechanical properties of the hydrogel. Knowledge of the formation and growth mechanisms of anisotropic polymer networks by self-assembly is expected to trigger innovations in the field of nanotechnology, including the fabrication of functional soft materials and self-organizing nanomaterials using bioinspired processes.

Author contributions

S. K., Y. N., and K. M. designed this study and developed the hypothesis. K. K., T. M., Y. N., and K. M. performed sample characterization. All authors discussed the results. All authors have read and approved the submitted manuscript.

Conflicts of interest

There are no conflicts to declare.

Acknowledgements

We would like to thank Editage (<https://www.editage.jp>) for English language editing.

Notes and references

- 1 T. Nonoyama, Y. W. Lee, K. Ota, K. Fujioka, W. Hong and J. P. Gong, *Adv. Mater.*, 2019, **32**, 1905868.
- 2 S. Xia, Q. Zhang, S. Song, L. Duan and G. Gao, *Chem. Mater.*, 2019, **31**, 9522–9531.
- 3 S. Sun, L.-B. Mao, Z. Lei, S.-H. Yu and H. Cölfen, *Angew. Chem., Int. Ed.*, 2016, **55**, 11765–11769.
- 4 T. Matsuda, R. Kawakami, R. Namba, T. Nakajima and J. P. Gong, *Science*, 2019, **363**, 504–508.
- 5 T. Karino, Y. Okumura, K. Ito and M. Shibayama, *Macromolecules*, 2004, **37**, 6177–6182.
- 6 M. A. Haque, T. Kurowaka, G. Kamita and J. P. Gong, *Macromolecules*, 2011, **44**, 8916–8924.
- 7 H. N. Kim, A. Jiao, N. S. Hwang, M. S. Kim, D. H. Kang, D.-H. Kim and K.-Y. Suh, *Adv. Drug Delivery Rev.*, 2013, **65**, 536–558.
- 8 Z. Zhao, R. Fang, Q. Rong and M. Liu, *Adv. Mater.*, 2017, **29**, 1703045.
- 9 X. Zhao, Q. Lang, L. Yildirim, Z. Y. Lin, W. Cui, N. Annabi, K. W. Ng, M. R. Dokmeci, A. M. Ghammaghami and A. Khademhosseini, *Adv. Healthcare Mater.*, 2016, **5**, 108–118.
- 10 A. Rosemary, O. H. Zhang, J. Chen, Y. Zhou, R. Wang, J. Fu, P. Müller-Buschbaum and Q. Zhong, *ACS Appl. Mater. Interfaces*, 2021, **13**, 22902–22913.

- 11 X. Yuan, Z. Zhu, P. Xia, Z. Wang, X. Zhao, X. Jiang, T. Wang, Q. Gao, J. Xu, D. Shan, B. Guo, Q. Yao and Y. He, *Adv. Sci.*, 2023, **10**, 2301665.
- 12 Z. Yang, L. Chen, D. J. McClements, C. Qiu, C. Li, Z. Zhang, M. Miao, Y. Tian, K. Zhu and Z. Jin, *Food Hydrocolloids*, 2022, **124**, 107218.
- 13 K. Kawaguchi, S. Komatsu, A. Kikuchi, Y. Nomura and K. Murai, *Polym. J.*, 2021, **54**, 377–383.
- 14 K. Murai, *Polym. J.*, 2023, **55**, 817–827.
- 15 R. Tsuchiya and K. Murai, *Mol. Syst. Des. Eng.*, 2022, **7**, 1602.
- 16 K. Murai, K. Inagaki, C. Hiraoka, S. Minoshima, T. Kinoshita, K. Nagata and M. Higuchi, *CrystEngComm*, 2019, **21**, 3557.
- 17 Y. Xu, F. Nudelman, E. D. Eren, M. J. M. Wirix, B. Cantaert, W. H. Nijhuis, D. Hermida-Merino, G. Portale, P. H. H. Bomans, C. Ottman, H. Friedrich, W. Bras, A. Akiva, J. P. R. O. Orgel, F. C. Meldrum and N. Sommerdijk, *Nat. Commun.*, 2020, **11**, 5068.
- 18 K. He, M. Sawczyk, C. Liu, Y. Yuan, B. Song, R. Deivanayagam, A. Nie, X. Hu, V. P. Dravid, J. Lu, C. Sukotjo, Y.-P. Lu, P. Král, T. Shokuhfar and R. Shahbazian-Yassar, *Sci. Adv.*, 2020, **6**, eaaz7524.
- 19 K. Murai, T. Kinoshita, K. Nagata and M. Higuchi, *Langmuir*, 2016, **32**, 9351–9359.
- 20 B. Cantaert, D. Kuo, S. Matsumura, T. Nishimura, T. Sakamoto and T. Kato, *ChemPlusChem*, 2017, **82**, 107–120.